RSC Advances

ROYAL SOCIETY OF CHEMISTRY

www.rsc.org/advances

Journal Name

RSCPublishing

COMMUNICATION

Dynamic Electrochemical Impedance Spectroscopy (DEIS) Studies of AZ31 Magnesium Alloy in Simulated Body Fluid Solution

Cite this: DOI: 10.1039/x0xx00000x

Received 00th January 2012,
Accepted 00th January 2012

DOI: 10.1039/x0xx00000x

www.rsc.org/

A. Srinivasan[a, b], Kwang Seon Shin[b], N. Rajendran*[a]

This study investigates the passive film formation and its breakdown on to AZ31 Mg alloy in simulated body fluid solution using dynamic electrochemical impedance spectroscopy (DEIS). The change in impedance values as a function of applied potential indicated the transformation of Mg from its passive to active state and dissolution.

Development of magnesium and its alloys with low aluminium content as biodegradable implant materials is one of the promising areas in current research. [1-8] Since Mg and its alloys have similar mechanical properties as that of the natural bone, they significantly reduce the stress shielding effect and enhance bone mineralization.[9] However, Mg is one of the chemically active materials and easily corrodes when it is in contact with aqueous environment and hence limits its application.[10-13] Atmospheric humidity is sufficient to oxidize Mg into magnesium hydroxides/oxides. The protection provided by this film against corrosion is limited because the formed film is no longer stable in chloride containing environment, immediately reacts with Cl^- present in the solution and is converted to soluble $MgCl_2$. [1, 14, 15]

It is important to study the several stages involved in the corrosion of Mg to understand their surface chemistry[16-18]. DEIS is one of the recently used electrochemical techniques to study passivation, pit initiation, propagation and degradation of metallic materials.[19-22] The effect of pH on the corrosion behaviour of pure Mg in 0.1 N NaCl solution using DEIS has recently been studied by Darowicki et al.[23] There are hardly any reports on the study of corrosion behaviour of AZ31 Mg in physiological medium using DEIS. The present study investigates the electrochemical corrosion behaviour of AZ31 Mg in SBF solution using DEIS. Potentiodynamic (PDP) and potentiostatic polarization studies have also been carried out to explore the distinct behaviour of AZ31 Mg alloy at cathodic and anodic regions. Change in chemical composition was analyzed using energy dispersive X-Ray analysis (EDAX). Surface morphology of AZ31 Mg polarized at different potential regions was also analysed using optical microscopy (OM).

AZ31 Mg alloy (2.83 wt. % Al, 0.8 wt. % Zn, 0.37 wt. % Mn, and balance Mg) was used as substrate material. Prior to carrying out the electrochemical measurements, AZ31 Mg samples (20 x 15 x 4 mm) were ground up to 2000# silicon carbide (SiC) emery papers, ultrasonicated in acetone for 15 min. The samples were then thoroughly washed with double distilled (DD) water, air dried and used for electrochemical studies.

Electrochemical measurements were carried out in a conventional three electrode flat cell and AZ31 Mg was used as working electrode (1 cm^2). Saturated calomel electrode (SCE) and Pt sheet were used as reference and counter electrodes, respectively. SBF solution reported by Kokubo et al.[24] was used as electrolyte. Auto lab PGSTAT 12 Potentiostat/Galvanostat, The Netherlands was used for DEIS and PDP and potentiostatic polarization studies. PDP study was carried out in the potential region from open circuit potential (OCP) - 0.050 V to several mV after breakdown potential at a scan rate of 1 mV/s. DEIS studies were carried out with an increment of 30 mV potential in the same potential range used for PDP studies. The frequency range was 100 kHz to 0.01 Hz with sinusoidal amplitude of 10 mV. Potentiostatic polarization measurement was carried out at constant potential for 600 s. JEOL-JSM 6360 scanning electron microscope attached with INCA X-Sight Oxford Instruments EDAX analyzer was used to obtain the surface chemical composition. The surface morphology of the samples after potentiostatic polarization was observed using Nikon P-III, OM model in bright field mode.

PDP curve of AZ31 Mg after 1 hour of exposure in SBF solution is shown in Fig. 1. The obtained polarization curve can be broadly divided into two major regions viz., (i) cathodic and (ii) anodic regions. The anodic region includes passive and break down regions. The possible electrochemical reaction in the cathodic region is hydrogen evolution ($H^+ + e^- \rightarrow ½\ H_2 \uparrow$). In most of the corrosion experiments the anodic region is more important rather than cathodic region because the metal surface undergoes different transformations there starting from passive to breakdown region ($Mg \rightarrow Mg^{2+} + 2e^-$ and $Mg^{2+} + 2(OH^-) \rightarrow Mg(OH)_2$). Hence, the anodic region is more focused to explain the corrosion behaviour of AZ31 Mg in SBF solution. As seen in Fig.1, the corrosion potential of AZ31 Mg in SBF solution is about -1.61 V, where both anodic and cathodic reactions are at equilibrium. However, upon increasing the potential in the anodic direction, the current density was slowly increasing up to -1.38 V. It is clear from the result that the region between -1.61 V

and -1.38 V is attributed to the passive region due to the formation of Mg $(OH)_2$. When the potential above -1.38 V, the anodic current density suddenly increased, indicating that the breakdown of the passive film. The increase in current density was recorded with further increase in anodic potential also confirming the pit growth and severe corrosive attack of the substrate AZ31 Mg in SBF solution. From the results it was possible to identify the potential regions of passive film formation and break down of AZ31 Mg in SBF solution.

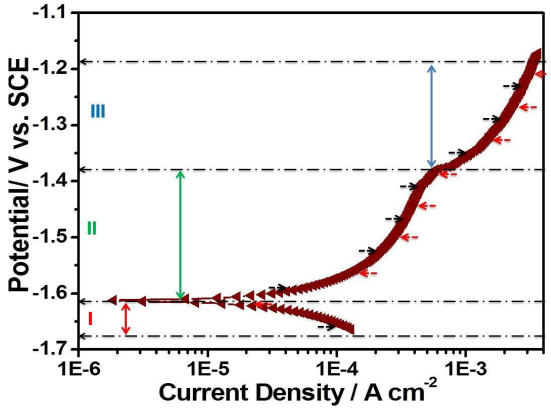

Fig. 1 Potentiodynamic polarization curve of AZ31 Mg alloy in SBF solution (I- Cathodic region, II-Passive region and III-Breakdown region).

Nyquist plots obtained under potentiodynamic condition in SBF solution are given in Fig. 2 (a-d). It is seen from the Fig. 2a that two depressed capacitive semicircles were obtained when the applied potential is between -1.65 and -1.62 V. It clearly indicates the existence of two different interfaces between AZ31 Mg and SBF solution. The capacitive semicircle appearing at high frequency region is attributed to the surface film/ SBF solution interface and low frequency capacitive semicircle is due to charge transfer between the film and metal interface. There is no inductive loop in low frequency region which indicates the absence of electrolyte diffusion at film/metal interface.

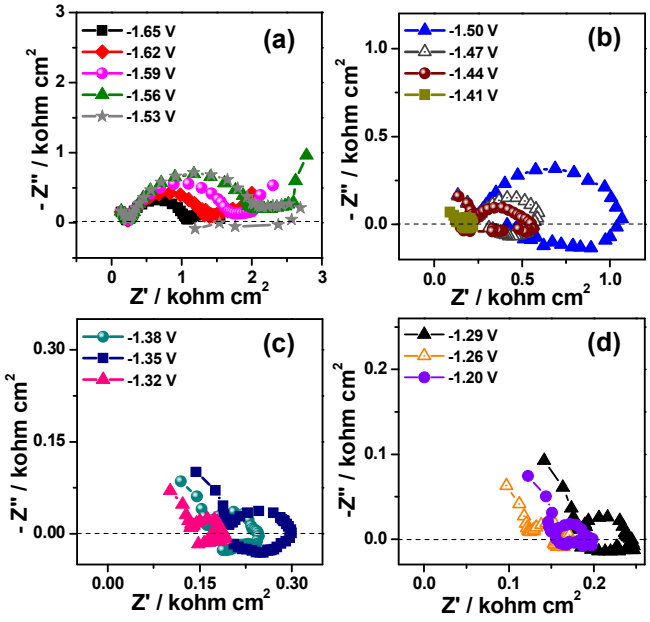

Fig. 2 Nyquist plots of AZ31 Mg in SBF solution as a function of applied potential.

Increasing the potential up to -1.53 V (Fig. 2a), increases the diameter of the high frequency capacitive semicircle. This indicates the increase of impedance value, which is due to the existence of passive film and it hinders the ingress of aggressive ions into the metal surface thereby lower the kinetics of corrosion process.[16] It is also presumed that the Al present in the alloy also would participate in the passive layer formation and that could stabilise the passive layer. [25, 26] Further the appearance of inductive loop at -1.53 V indicating the adsorption of corrosive ions. However the capacitive semicircle at high frequency region vanished when the applied potential is increased above -1.53 V and only one capacitive semicircle with inductive loop at low frequency was visible (Fig. 2b). The diameter of the capacitive semicircle subsequently was reduced and also the inductive loop was predominant as a function of anodic potential. The absence of high frequency semi-circle indicated the degradation of passive film. Further, the appearance of well distinguished inductive loop at -1.50 V confirmed the onset of corrosive ions diffusion at the interface and is a direct evidence for the initiation of corrosion at the metal surface. The disappearance of high frequency capacitive semicircle and also the reduction in diameter of the semi-circle indicated the reduction in charge transfer resistance (R_{ct}) and increase in the Mg dissolution kinetics. The change in the nature of semi-circle with variation in the applied potential clearly depicted the transformation of passive to active state.

The diameter of the capacitive semicircle was continuously reducing with increasing anodic potential, indicating the severe attack of the corrosive ions on the surface of the alloy. It is also seen form Fig. 2c and d that increasing the potential above -1.38 V results in significant reduction of impedance value and the diffusion of electrolyte into the film/ metal interface was predominant due to the intense micro galvanic corrosion within the alloy. [27] DEIS studies of pure Mg by Orlikowski et al [23] in 0.1 M NaCl solution with varying pH does not show any sign for the appearance of inductive loop even with increasing the potential. The appearance of well distinguished inductive loop in the present study with increasing potential could be due to the detrimental effect of the alloying elements. These results further confirming the complete breakdown of the passive film from the surface and accelerate the degradation rate of AZ31 Mg in SBF solution.

In order to further explain the corrosion behaviour of AZ31 Mg using DEIS, the obtained results were curve fitted using equivalent circuit (EC) models (Fig. 3 a-c) and the derived EC parameters are compared and given in Fig. 4 a-c. The fitting error between the measured and calculated values was about 5%.

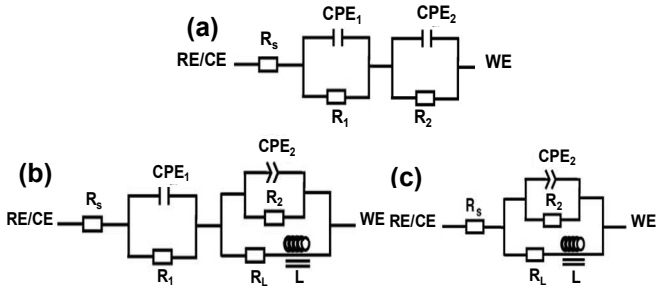

Fig. 3 Equivalent circuit models used for curve fitting of DEIS results. (a) -1.65 to -1.56 V: (b) -1.53 V and (c) -1.50 to -1.20 V. RE - Reference electrode, CE - Counter electrode and WE- Working electrode. R_s- Solution resistance, R_1 and R_2 - Surface film and charge transfer resistance. CPE_1 and CPE_2 - Constant phase elements of surface film and double layer. R_L and L - Inductive resistance and L - Inductance.

Since there is a significant difference in Nyquist plots obtained as a function of applied potential, three different equivalent circuit models have been proposed and used to analyse the obtained impedance results. EC model depicted in Fig.3a was used for the fitting of Nyquist plots obtained between -1.65 to -1.56 V. R_1 and R_2 values increased with increasing potential from -1.65 to -1.56 V is the direct evidence for the formation of passive film on to the surface. Decreasing trend in CPE_1 and CPE_2 values in the same potential region are also further supporting the passive film formation (Fig. 4b). When the applied potential increased to -1.53 V as can be seen in the Nyquist plot, the inductive loop was appeared along with two capacitive semi circles. Hence the circuit element corresponding to inductive loop (R_L and L) was introduced in Fig.3a and suitably modified as show in Fig.3b. [28] This EC model would be more appropriate for curve fitting of Nyquist plot at-1.53V. R_L and L values are high at -1.53V (Fig. 4c) clearly indicating adsorption of corrosive ions and onset of pit initiation. Further increase in applied potential resulted in the disappearance of high frequency capacitive semi circle is due to the breakdown of the passive film. Therefore the EC model in Fig. 3c was used when the applied potential exceeds -1.53 V. It is noticed from Fig. 4 a & b that the R_2 value decreased and CPE_2 value increased with increasing the potential confirming the Mg dissolution. Further, the R_L and L values also exhibited decreasing trend with increasing potential revealed the acceleration of Mg dissolution.

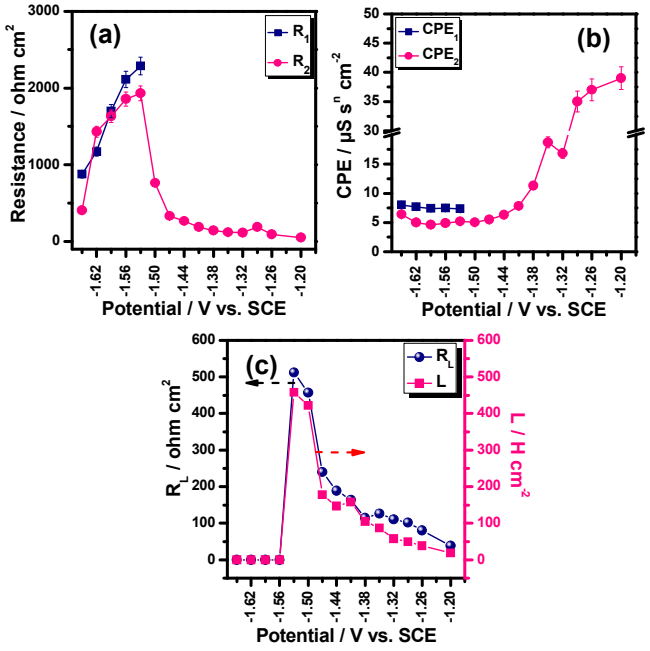

Fig. 4 Comparison of EC parameters derived from Nyquist plots.

The change in current density was measured in SBF solution as a function of potential and given in Fig. 5. The current density was found to be about 0.001 A cm^{-2} after 600 s at -1.65 V in SBF solution. Increasing the potential up to -1.44 V, results in increasing the current density to 0.002 A cm^{-2} which is about two times when compared to the current density at -1.65 V. When the applied potential was increased between -1.44 to -1.20 V, the current density was also increased to about 0.005 A cm^{-2} at -1.20 V. The slow increase (0.001 A cm^{-2}) in current density up to -1.44 V is due to the presence of passive film on the surface. However, the formed film is no longer stable when the applied potential is increased further and breaks to allow the corrosive ions to penetrate through the film to metal surface thereby rapidly increasing the current density to 0.005 A cm^{-2}. By careful analysis of the results it is seen that the change in current density was found to be 0.001 and 0.005 A cm^{-2} for the potential range of -1.65 to -1.44 V and -1.44 to -1.20 V respectively.

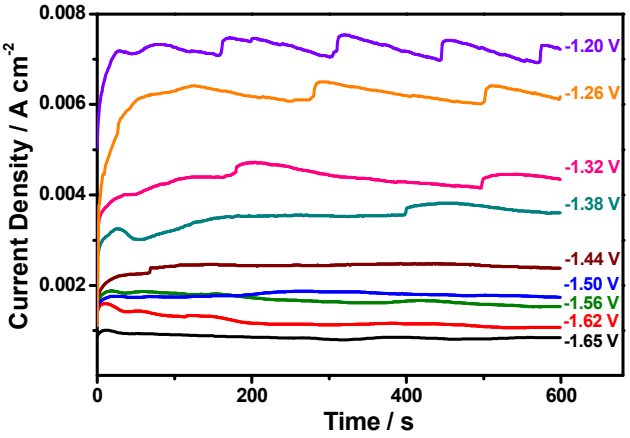

Fig. 5 Change in current density values of AZ31 Mg in SBF solution with potential.

Change in surface chemical composition of AZ31 Mg after potentiostatic polarization has been analyzed using EDAX and are given in the Fig. 6. The amount of O was slowly increased and Mg was decreased as the applied potential increased up to -1.44 V (Fig.6a). When the potential increased above -1.44 V the amount of O was suddenly increased and Mg content drastically reduced. These results confirmed the formation of passive film and its breakdown with potential. It is interesting to note that when the applied potential increased upto -1.44 V slight increase of Al content is attributed to the participation of Al in passive film formation. Further increase in applied potential resulted in sudden increase of Al and Zn content on the surface indicating the enrichment of these elements in the loosely bound corrosion product on the surface of AZ31 Mg due to corrosion. No significant difference was noticed in the Mn content with increasing potential. EDAX composition analysis clearly indicated the change of surface composition due to the Mg corrosion and also the influence of alloying elements on the corrosion behaviour of AZ31 Mg as a function of applied potential.

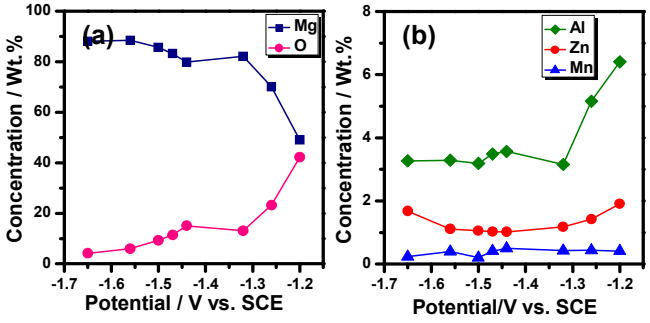

Fig. 6 Change in chemical composition of AZ31 Mg subjected to potentiostatic polarization in SBF solution for 600 s.

The optical microscopic images of polarized samples are given in Fig. 7. The pit formation and propagation was not well distinguished until the potential was -1.44 V and above -1.44 V the pit formation and growth were well distinguished. In particular when the potential reached above -1.32 V the pit growth was seen thus directly confirming the severe attack of AZ31 Mg in SBF solution.

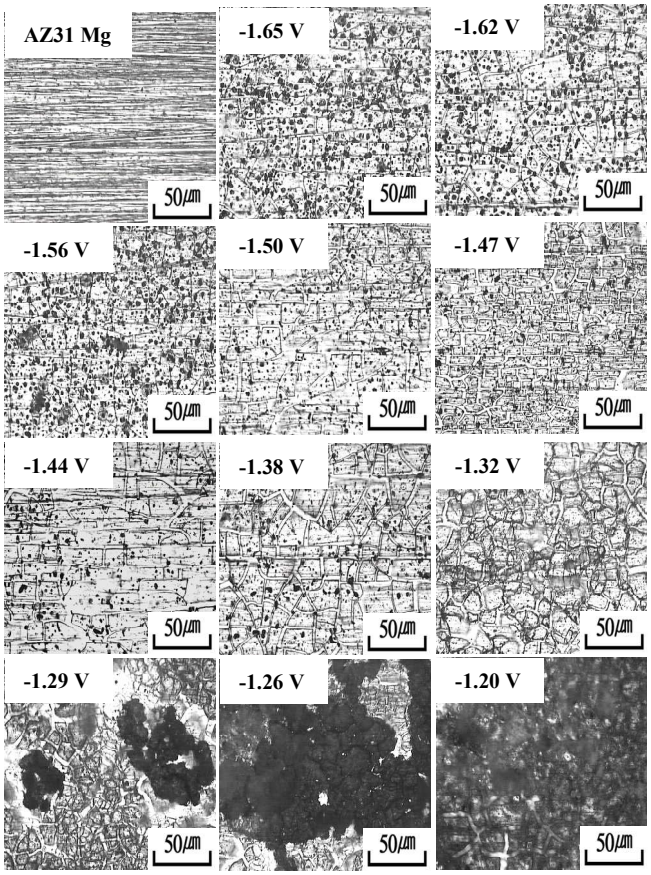

Fig. 7 Optical micrographs of AZ31 Mg after potentiostatic polarization studies in SBF solution.

In summary the electrochemical corrosion behaviour of AZ31 Mg alloy in SBF solution has been carried out. Potentiodynamic polarization studies helped to identify potential at which the passive film formation and break down processes occur. DEIS studies confirmed the existence of passive film and change in charge transfer resistance value as a function of applied potential. The complete breakdown of the passive film was ensured from the disappearance of high frequency capacitive semicircle with predominant inductive loop at low frequency region. Equivalent circuit parameters derived from DEIS results and EDAX chemical composition are also substantiated the results. About 2.5 times increase in current density in potentiostatic polarization studies was evidenced from -1.44 V to -1.20 V and was attributed to breakdown of the passive film and severe corrosive attack was further supported by the optical microscopic studies. Hence DEIS could be a useful technique to understand the Mg corrosion for biomedical applications in future.

The authors A. S and N. R acknowledge the financial assistance received from the Department of Science and Technology - Science and Engineering Research Board (DST-SERB), New Delhi (SR-SP-01-14, Dt.08.02.2011). Author KSS acknowledge WPM Program, funded by the Korean Ministry of Trade, Industry and Energy through the Research Institute of Advanced Materials. The facilities provided by DST-FIST and UGC-DRS are also gratefully acknowledged.

Notes and references

[a] Department of Chemistry, College of Engineering Guindy Campus, Anna University, Chennai-600 025, Tamilnadu, India.
[b] Magnesium Technology Innovation Center, School of Materials Science and Engineering, Seoul National University,1 Gwanak-ro, Gwanak-gu, Seoul-151-744, Republic of Korea.

1. Y. Xin, T. Hu, P. K. Chu, *Acta Biomater.* 2011, **7**, 1452.
2. F. Witte, N. Hort, C. Vogt, S. Cohen, K. U. Kainer, R. Willumeit, F. Feyerabend, *Curr. Opin. Solid State Mater. Sci.* 2008, **12**, 63.
3. M. P. Staiger, A. M. Pietak, J. Huadmai, G. Dias, *Biomaterials* 2006, **27**, 1728.
4. S. Zhang, X. Zhang, C. Zhao, J. Li, Y. Song, C. Xie, H. Tao, Y. Zhang, Y. He, Y. Jiang, Y. Bian, *Acta Biomater.* 2010, **6**, 626.
5. H. Hermawan, D. Dubé, D. Mantovani, *Acta Biomater.* 2010, **6**, 1693.
6. K. S. Shin, H. C. Jung, M. Z. Bian, N. D. Nam, N. J. Kim, *European Cells and Mater.* 2013, **26 (5)**, 4.
7. H. S. Han, Y. Y. Kim, Y. C. Kim, S. Y. Cho, P. R. Cha, H. K. Seok, S. J. Yang, *Metals and Mater. Inter.* 2012, **18**, 243.
8. K. S. Shin, M. Z. Bian, N. D. Nam, JOM 2012, **65**, 1.
9. Y. Song, D. Shan, R. Chen, F. Zhang, En-Hou Han, *Mater. Sci. Eng. C* 2009, **29**, 1039.
10. Y. Xin, K. Huo, T. Hu, G. Tang, P. K. Chu, *J. Mater. Res.* 2009, **24**, 2711.
11. Y. Xin, T. Hu, P. K. Chu, *J. Electrochem. Soc.* 2010, **157**, C238.
12. Z. Li, G. L. Song, A. Song, *Electrochim. Acta* 2014, **115**, 56.
13. N. I. Z. Abidin, A. D. Atrens, D. Martin, A. Atrens, *Corros. Sci.* 2011, **53**, 3542.
14. Y. Wang, C. S. Lim, M. S. Yong, E. K. Teo, L. N. Moh, *Mater. Sci. Eng. C* 2011, **31**, 579.
15. G. L. Song, A. Atrens, *Adv. Eng. Mater.* 1999, **1**, 11.
16. J. H. Jo, B. G. Kang, K. S. Shin, H. E. Kim, B. D. Hahn, D. S. Park, Y. H. Koh, *J. Mater. Sci.: Mater. in Medicine* 2011, **22**, 2437.
17. J. H. Jo, J. Y. Hong, K. S. Shin, H. E. Kim, Y. H. Koh, *J. Biomater. Appl.* 2011, **27(4)**, 469.
18. Y. K. Kim, I. S. Park, S. J. Lee, M. H. Lee, *Metals and Mater. Inter.* 2013, **19**, 353.
19. K. Darowicki, J. *Electroanal. Chem.* 2000, **486**, 101.
20. K. Darowicki, S. Krakowiak, P. Slepski, *Electrochim. Acta* 2004, **49**, 2909.
21. S. Nagarajan, M. Karthega, N. Rajendran, *J Appl. Electro. Chem.* 2007, **37**, 195.
22. W. C. Kim, K. H. Han, J. G. Kim, S. J. Yang, H. K. Seok, H. S. Han, Y. Y. Kim, *Metals and Mater. Inter.* 2013, **19**, 1131.
23. J. Orlikowski, K. Darowicki, *Electrochim. Acta* 2011, **56**, 7880.
24. T. Kokubo, H. Takadama, *Biomaterials* 2006, **27**, 2907.
25. M. Alvarez-Lopez, M. D. Pereda, J. A. Del Valle, M. Fernandez-Lorenzo, M. C. Garcia-Alonso, O. A. Ruano, M. L. Escudero, *Acta Biomater.* 2010, **6**, 1763.
26. G. Baril, C. Blanc, N. Pebere, *J Electrochem. Soc.* 2001, **148**, B489.
27. Y. Xin, C. Liu, X. Zhang, G. Tang, X. Tian, P. K. Chu, *J Mater. Res.* 2007, **22**, 2004.
28. A. Srinivasan, P. Ranjani, N. Rajendran, *Electrochim. Acta* 2013, **88**, 310.

TOC:

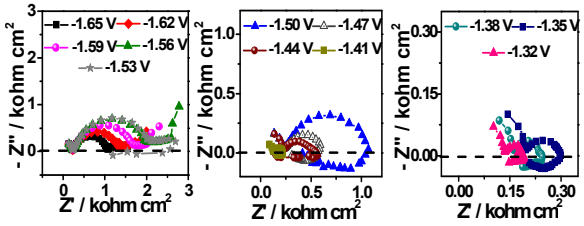

The change in impedance values as a function of potential indicated the transformation of Mg from its passive to active state.